Pervasive non-additive and interaction effects in the HLA modulate the risk of autoimmune diseases

Tobias L. Lenz[1-3,*], Aaron J. Deutsch[1,2,4-7,*], Buhm Han[1,2,4-6,8], Xinli Y. Hu[1,2,4-7], Yukinori Okada[1,2,4-6,9,10], Stephen Eyre[11,12], Michael Knapp[13], Alexandra Zhernakova[14], Tom W.J. Huizinga[15], Goncalo Abecasis[16], Jessica Becker[17,18], Guy E. Boeckxstaens[19], Wei-Min Chen[20], Andre Franke[21], Dafna D. Gladman[22-24], Ines Gockel[25], Javier Gutierrez-Achury[14], Javier Martin[26], Rajan P. Nair[27], Markus M. Nöthen[17,18], Suna Onengut-Gumuscu[20], Proton Rahman[28], Solbritt Rantapää-Dahlqvist[29], Philip E. Stuart[27], Lam C. Tsoi[16], David A. van Heel[30], Jane Worthington[11,12], Mira M. Wouters[19], Lars Klareskog[31], James T. Elder[27,32], Peter K. Gregersen[33], Johannes Schumacher[17,18], Stephen S. Rich[20], Cisca Wijmenga[14], Shamil R. Sunyaev[1,2,6], Paul I.W. de Bakker[34,35], Soumya Raychaudhuri[1,2,4-6,36]

1. Division of Genetics, Department of Medicine, Brigham and Women's Hospital, Boston, MA, USA
2. Harvard Medical School, Boston, MA, USA
3. Evolutionary Immunogenomics, Department of Evolutionary Ecology, Max Planck Institute for Evolutionary Biology, Ploen, Germany
4. Division of Rheumatology, Immunology and Allergy, Department of Medicine, Brigham and Women's Hospital, Boston, MA, USA
5. Partners Center for Personalized Genetic Medicine, Boston, MA, USA
6. Program in Medical and Population Genetics, Broad Institute of MIT and Harvard, Cambridge, MA, USA
7. Harvard-MIT Division of Health Sciences and Technology, Boston, MA, USA
8. Asan Medical Center, Seoul, Korea
9. Department of Human Genetics and Disease Diversity, Graduate School of Medical and Dental Sciences, Tokyo Medical and Dental University, Tokyo, Japan
10. Laboratory for Statistical Analysis, RIKEN Center for Integrative Medical Sciences, Yokohama, Japan
11. Arthritis Research UK Centre for Genetics and Genomics, Centre for Musculoskeletal Research, University of Manchester, Manchester Academic Health Sciences Centre, Manchester, UK
12. NIHR Manchester Musculoskeletal Biomedical Research Unit, Central Manchester University Hospitals NHS Foundation Trust, Manchester Academic Health Sciences Centre, Manchester, UK
13. Institute for Medical Biometry, Informatics, and Epidemiology, University of Bonn, Bonn, Germany
14. Genetics Department, University Medical Centre Groningen and University of Groningen, Groningen, The Netherlands
15. Department of Rheumatology, Leiden University Medical Centre, Leiden, Netherlands
16. Department of Biostatistics and Center for Statistical Genetics, University of Michigan, Ann Arbor, MI, USA

17. Institute of Human Genetics, University of Bonn, Bonn, Germany
18. Department of Genomics, Life & Brain Center, University of Bonn, Bonn, Germany
19. Translational Research Center for Gastrointestinal Disorders, KULeuven, Leuven, Belgium
20. Center for Public Health Genomics, University of Virginia, Charlottesville, VA, USA
21. Institute of Clinical Molecular Biology, Kiel University, Kiel, Germany
22. Division of Rheumatology, Department of Medicine, University of Toronto, Toronto, ON, Canada
23. Centre for Prognosis Studies in the Rheumatic Diseases, Toronto Western Research Institute, University of Toronto, Toronto, ON, Canada
24. Toronto Western Research Institute, University of Toronto, Toronto, ON, Canada
25. Department of Visceral, Transplant, Thoracic and Vascular Surgery, University Hospital of Leipzig, Germany
26. Instituto de Parasitologia y Biomedicina Lopez-Neyra, Consejo Superior de Investigaciones Cientificas, Granada, Spain
27. Department of Dermatology, University of Michigan Medical School, Ann Arbor, MI, USA
28. Memorial University of Newfoundland, St. John's, NL, Canada
29. Department of Public Health and Clinical Medicine and Department of Rheumatology, Umea University, Umea, Sweden
30. Blizard Institute, Barts and The London School of Medicine and Dentistry, Queen Mary University of London, London, UK
31. Rheumatology Unit, Department of Medicine, Karolinska Institutet and Karolinska University Hospital Solna, Stockholm, Sweden
32. Ann Arbor Veterans Affairs Hospital, Ann Arbor, MI, USA
33. The Feinstein Institute for Medical Research, North Shore–Long Island Jewish Health System, Manhasset, NY, USA
34. Department of Medical Genetics, University Medical Center Utrecht, Utrecht, Netherlands
35. Department of Epidemiology, University Medical Center Utrecht, Utrecht, Netherlands
36. Faculty of Medical and Human Sciences, University of Manchester, Manchester, UK

* These authors contributed equally to this work.

Corresponding authors:

Soumya Raychaudhuri
Harvard New Research Building, Suite 250D
77 Avenue Louis Pasteur
Boston, MA 02446, United States of America
soumya@broadinstitute.org

Tel: +1 617-525-4484
Fax: +1 617-525-4488

Paul I.W. de Bakker
University Medical Center Utrecht
Stratenum 0.310
PO Box 85500
3508 GA Utrecht, The Netherlands
pdebakker@umcutrecht.nl
Tel: +31 887550406
Fax: +31 887555410

Format: Nature Genetics Letter
Organization: Introductory paragraph, main text, 2 tables, 3 figures, supplementary materials
Keywords: Autoimmunity, complex diseases, MHC, HLA, genetic architecture, non-additive effects, interaction

INTRODUCTORY PARAGRAPH

Human leukocyte antigen (HLA) genes are strongly associated with risk of autoimmune diseases. While current models commonly assume log-additive effects, we speculated that differences in autoantigen binding repertoires between a heterozygote's two expressed HLA variants may result in non-additive risk effects. We tested non-additive disease contributions of classical HLA alleles in 25,835 patients with rheumatoid arthritis (RA), type 1 diabetes (T1D), psoriasis vulgaris (PsV), idiopathic achalasia (Ach) or celiac disease (CeD), and matched controls. In four out of the five common autoimmune diseases, we observed highly significant non-additive terms (RA: $P = 2.5\text{x}10^{-12}$; T1D: $P = 2.4\text{x}10^{-10}$; PsV: $P = 5.9\text{x}10^{-6}$; CeD: $P = 1.2\text{x}10^{-87}$). In three of these diseases, the non-additive terms were explained by interactions between specific classical HLA alleles (RA: $P = 1.8\text{x}10^{-3}$, T1D: $P = 8.6\text{x}10^{-27}$; CeD: $P = 6.0\text{x}10^{-100}$), as opposed to dominance effects. These interactions generally increased disease risk and explained an additional 1.4% of phenotypic variance in RA, 4.0% in T1D, and 4.1% in CeD, beyond a simple additive model.

MAIN TEXT

Genetic variation within HLA genes, as part of the major histocompatibility complex (MHC), is associated with many autoimmune diseases, including rheumatoid arthritis and multiple sclerosis[1-3]. For these diseases, the MHC explains more phenotypic variance than any other locus does. Previous research has shown non-additive effects (*e.g.* overdominance) at classical MHC genes in resistance to infectious diseases[4-7], and researchers have proposed that non-additive effects may also occur in autoimmune diseases[8-12]. Indeed, some studies have reported synergistic interactions between certain HLA haplotypes[13-15], but non-additive effects and

interactions have not been systematically characterized in large cohorts and across multiple independent diseases.

In an additive model, the effects of two risk alleles combine linearly on the log-odds scale; non-additive effects arise from interactions between two alleles, or from intrinsic effects of individual alleles (*e.g.* due to haploinsufficiency)[16,17]. Since both alleles at a given HLA locus are expressed, heterozygous genotypes might confer expanded antigen binding properties and elevated autoantigen presentation, depending on the degree of complementarity between the two alleles[18]. As a result, interactions between HLA alleles (within the same locus or across separate loci) can yield non-additive effects.

In order to test for the presence of non-additive effects, we used SNP2HLA[19] to impute HLA alleles from dense ImmunoChip-based SNP genotype data in five autoimmune diseases: seropositive rheumatoid arthritis (RA, $N_{cases/controls}$ = 5,337/11,049)[20,21], type 1 diabetes (T1D, N = 5,567/6,265)[22], psoriasis vulgaris (PsV, N = 3,089/5,964)[23], idiopathic achalasia (Ach, N = 727/2,911)[24], and celiac disease (CeD, N = 11,115/9,042)[25] (**Supplementary Table S1**). We demonstrated accurate HLA imputation elsewhere[19] using the ImmunoChip platform and the same reference panel (T1D Genetics Consortium, N = 5,225)[26].

Based on recent studies that fine-mapped HLA associations to these five diseases, we focused our analyses of non-additive effects on four-digit classical alleles at the HLA loci with the strongest effects (RA: *HLA-DRB1*, T1D: *HLA-DRB1-DQA1-DQB1*, PsV: *HLA-C*, Ach: *HLA-DQA1-DQB1*, CeD: *HLA-DQA1-DQB1*). Since T1D, Ach, and CeD have independent associations to multiple, linked HLA genes[22,24,25], we

combined phased four-digit classical alleles from separate genes into multi-locus haplotypes for these diseases. For our primary test, we restricted our analysis to common alleles at each locus (reference panel allele frequency > 5%; **Supplementary Table S2**) and to individuals carrying only these common alleles ("common allele dataset", **Supplementary Table S1**). This approach ensured the highest imputation accuracy, and it increased the statistical power to estimate the true additive component of each haplotype by providing a sufficient number of homozygote events. As a secondary test, we analyzed both rare and common haplotypes that were present in at least 10 homozygous individuals ("full dataset", **Supplementary Table S1**).

To assess for non-additive associations, we first examined disease risk of homozygotes and heterozygotes for each haplotype. Under additivity, the log-odds of heterozygotes should be half that of homozygotes. However, we found that many haplotypes deviated from this linear relationship (**Figure 1a**). We also observed an excess of heterozygous genotypes outside of Hardy-Weinberg equilibrium in cases (**Figure 1b**), but not controls (**Figure 1c**). In contrast, 44 RA-associated non-MHC SNPs[27] followed an additive relationship perfectly (**Figure 1d**) and also followed Hardy-Weinberg equilibrium (**Figure 1e**). We note that the lower effect sizes of non-MHC variants may limit our ability to detect non-additive effects.

To test for the general presence of non-additive effects, we constructed one logistic regression model for each disease with additive and dominance terms for all common haplotypes (**Figure 2a**)[28]. Strikingly, for four of the five diseases, the inclusion of dominance terms improved the fit of the models (RA: $P_{df=5} = 2.5\text{x}10^{-12}$; T1D: $P_{df=5} = 2.4\text{x}10^{-10}$, PsV: $P_{df=7} = 5.9\text{x}10^{-6}$; CeD: $P_{df=6} = 1.2\text{x}10^{-87}$). In the achalasia dataset we

observed a non-significant trend ($P_{df=5}$ = 0.066); power may have been limited due to the relatively small sample size of this dataset. These results were consistent in the full datasets, including a larger set of common and rare alleles (**Supplementary Table S3**). In a purely additive model, common HLA haplotypes explained 8.1% of phenotypic variance for RA, 13.3% for T1D, 5.9% for PsV, and 21.1% for CeD. The addition of dominance terms explained an additional 0.9%, 1.1%, 0.9%, and 1.9% of phenotypic variance, respectively (**Figure 2b**). These values are comparable to the effect of the largest known non-MHC RA risk effect; the rs2476601 *PTPN22* risk allele explains 0.8% of the total phenotypic variance in RA[29].

When we examined non-additive effects of individual HLA haplotypes separately, we observed that most haplotypes showed significant non-additive contributions in RA, T1D, and CeD (**Table 1, Supplementary Table S6**). In contrast, of 7 common haplotypes tested in PsV, only HLA-*C*06:02* showed a non-additive effect. Across all four diseases, 14 of 23 HLA haplotypes showed non-additivity, and 12 had a positive dominance component; thus, for most alleles, heterozygosity confers a higher risk of autoimmunity than expected from homozygote disease risk (**Figure 2c**).

We considered the possibility that the observed non-additive effects might have arisen from imputation artifacts. In order to ensure high quality imputation, we only used samples genotyped on ImmunoChip, which contains dense SNP coverage (>5,000 SNPs within the MHC)[19]. We also imputed cases and controls together, to ensure consistent imputation quality across all samples. Additionally, our primary analyses focused on common alleles that were well represented in the reference panel and had high imputation confidence (INFO) scores[30] (>0.973, median 1.003, **Supplementary Table S2**). We note that *P*-values for non-additive effects were

unrelated to INFO scores (Kendall's *tau* = -0.08, *P* = 0.56; **Supplementary Fig. S1**). Finally, we conducted a stringent permutation analysis where we reassigned case-control status, based on an additive risk model for HLA haplotypes, and then assessed if non-additive effects were spuriously observed. This approach conserved the additive effect of each haplotype (**Supplementary Figure S3)** and simultaneously maintained any imputation inaccuracies within the dataset. Across all four diseases with significant non-additive effects, the fit of the dominance model in 10,000 trials never exceeded the fit observed in the actual data (**Supplementary Figure S4**). These results argue that our findings cannot be explained by imputation artifacts.

In RA, T1D, and Ach, the strongest additive disease associations point to individual amino acids (rather than four-digit classical alleles)[20,22,24]. Nonetheless, non-additive haplotype effects remained significant even after controlling for the non-additive effects of individual amino acids (**Supplementary Note S1**).

We then investigated whether interactions between specific haplotypes might explain the non-additive dominance effects; interactions are present when disease risk for specific pairs of haplotypes deviates from a linear relationship. We defined a logistic regression model that included first-order interaction terms between all common haplotypes within a given locus. For three diseases (RA, T1D, and CeD), which are most strongly associated with HLA class II genes, the model with additive terms and interaction terms showed a significant improvement in fit, compared to a model with additive and dominance terms (RA: $P_{df=5} = 1.8x10^{-3}$, T1D: $P_{df=5} = 8.6x10^{-27}$; CeD: $P_{df=9} = 6.0x10^{-100}$). Hence, the observed non-additive effects for RA, T1D, and CeD are at least partially explained by interactions between HLA haplotypes. The models with

additive and interaction terms explained 9.45%, 17.31%, and 25.22% of phenotypic variance for RA, T1D, and CeD, respectively; interactions yielded an additional 0.46%, 2.94%, and 2.25% of phenotypic variance over a model with additive and dominance terms (**Figure 2b**).

In contrast, PsV (most strongly associated with a HLA class I gene, HLA-C) showed no evidence of interactions ($P_{df=14}$ = 0.92). In order to further identify interactions, we imputed an additional 5,294 psoriasis cases and 10,295 controls genotyped on platforms other than ImmunoChip (**Supplementary Table S1c**). While this increased our sample size dramatically, we still observed no evidence of interactions ($P_{df=14}$ = 0.87; **Supplementary Table S10**). The contrast between PsV and other diseases may be related to recent suggestions that the PsV association with HLA-C*06:02 is caused by variation in an HLA-C*06:02 expression-controlling enhancer element[31], rather than antigenic binding properties. Ach showed no evidence for interaction effects in our primary analysis ($P_{df=5}$ = 0.15), and only nominal evidence when we tested the full dataset with common and rare haplotypes. All other diseases yielded qualitatively identical results when we tested the full datasets with both rare and common haplotypes (**Supplementary Table S3**).

We then identified the specific HLA haplotypes contributing to interaction effects in RA, T1D, and CeD. For RA, 7 of the 10 possible interactions were significant (P<0.005=0.05/10), and all increased disease risk beyond the separate additive contribution of each haplotype (**Table 2, Fig. 3a**). For T1D, 7 of 10 interactions were significant (P<0.005=0.05/10), with five increasing risk and two reducing risk (**Supplementary Table S8, Supplementary Figure S5**); these interactions are detailed elsewhere and are included here for completeness[22]. For CeD, among the

15 possible haplotype pairs, there were four significant pairwise interactions (P<0.003=0.05/15), each increasing risk (**Table 2, Fig. 3b**). The identified interactions refined our previous findings of non-additive disease contributions. For instance, in CeD, DQA1*05:01-DQB1*02:01 had a significant non-additive component ($P = 4.7x10^{-19}$) with $d > 0$, indicating an elevated disease risk in heterozygotes. This elevated disease risk is explained by the interaction model, in which we observed significant risk-increasing interactions between DQA1*05:01-DQB1*02:01 and three other alleles (**Fig. 3b**).

Our results build on previous studies that proposed specific non-additive associations in different autoimmune diseases. While previous studies of heterozygote risk in RA focused on haplotypes with a common 'shared epitope' (SE) at positions DRβ1#70-74[32,33], we discovered significant interactions between SE haplotypes and non-SE haplotypes. There was no evidence for a previously reported interaction between DRB1*04:01 and DRB1*04:04[34] (**Supplementary Note S2**). A few specific interactions in T1D have been described previously, such as an elevated disease risk for HLA-DRB1*03-DQB1*02/DRB1*0401-DQB1*0302 genotypes[15]. Our recent comprehensive investigation of T1D also confirmed this interaction and revealed additional interactions with both increasing and decreasing risk effects[22].

In CeD, the DQ2.5 haplotype, consisting of the combination of HLA-DQA1*05:01 and HLA-DQB1*02:01, is the primary contributor to CeD susceptibility[35,36]. Here, we confirmed that DQA1*05:01-DQB1*02:01 has the strongest disease association in an additive model ($P = 4.3x10^{-675}$), and we also found significant interactions between DQA1*05:01-DQB1*02:01 and other haplotypes. Some of these combinations contained DQA1*05:01 and DQB1*02:01 in *trans*, but we also observed haplotype

combinations that have not previously been implicated (e.g. DQA1*05:01-DQB1*02:01/DQA1*01:01-DQB1*05:01; OR = 3.74, $P = 1.9x10^{-10}$). Interestingly, the interaction with the strongest risk effect in our data (DQA1*02:01-DQB1*02:02/DQA1*05:01-DQB1*03:01; OR = 16.85, $P = 7.0x10^{-74}$), identified in previous studies[37], contained the protective haplotype DQ7 (coded by DQA1*05:01-DQB1*03:01; homozygote OR = 0.03), highlighting the complexity of interactions in the HLA.

Interestingly, we note that there was little overlap between diseases in the pairs of haplotypes with significant interactions, suggesting that the precise interactions are disease specific. These interactions may depend on the exact autoantigens driving disease susceptibility[2]. Such a scenario would be consistent with previous observations, in particular in RA, where specific T and B cell reactions against different citrullinated autoantigens seem to be restricted by different HLA-DR variants involving different immune effector functions[38,39]. Similarly, in CeD, where the major disease antigen is known, expression of the gluten peptide-presenting HLA-DQ2.5 variant is the primary determinant of disease risk, which can be formed by genotypes carrying HLA-DQA1*05:01 and HLA-DQB1*02:01 in *trans*, explaining the observed interaction effect between these haplotypes[36]. Another possibility is that differential intrinsic stability of certain *trans*-heterodimers may also affect disease risk, as suggested for HLA-DQ in T1D[40]. Further investigations of causal mechanisms are needed to precisely understand how interacting alleles confer genetic predisposition for these complex diseases.

Acknowledgments

This project was supported by grants from the German Research Foundation (DFG, LE 2593/1-1 and LE 2593/2-1 (TLL), GO 1795/1-1 (IG), KN 378/2-1 (MK), SCHU 1596/5-1 (JS)), by NIH grants (1R01AR062886, R01AR065183, 1R01AR063759-01A1, and 5U01GM092691 (SR)), by the IMI (EU)-funded program BTCure (LK). Sample collection of JM was supported by a grant from the Instituto de Salud Carlos III (RD12/0009). MMN received support for this work from the Alfried Krupp von Bohlen und Halbach-Stiftung and is a member of the DFG funded Excellence Cluster ImmunoSensation.

Author Contributions

TLL, AJD, SR, PIWdB, and SRS conceived the study, coordinated the study, and wrote the initial version of the manuscript. TLL, AJD, SR, BH, XH, YO, PIWdB and SRS contributed to the study design and analysis strategy. All analyses were conducted by TLL, AJD, and SR. The following authors organized and contributed subject samples and provided SNP genotype data; for RA: SE, TWJH, LK, JM, SR-D, JW, and PG; for T1D: W-MC, SO-G, and SSR; for PsV: GA, AF, DDG, RPN, PR, PES, LCT, and JTE; for CeD: JG-A, DAVH, AZ, and CW; for Ach: JB, GEB, IG, MK, MMN, MMW, and JS. All authors contributed to writing the final manuscript.

Competing Financial Interests

The authors declare no competing financial interests.

References

1. Horton, R. *et al.* Gene map of the extended human MHC. *Nat. Rev. Genet.* **5**, 889-899 (2004).
2. Parkes, M., Cortes, A., van Heel, D.A. & Brown, M.A. Genetic insights into common pathways and complex relationships among immune-mediated diseases. *Nat. Rev. Genet.* **14**, 661-673 (2013).
3. Trowsdale, J. & Knight, J.C. Major histocompatibility complex genomics and human disease. *Annu. Rev. Genomics Hum. Genet.* **14**, 301-323 (2013).
4. Thursz, M.R., Thomas, H.C., Greenwood, B.M. & Hill, A.V. Heterozygote advantage for HLA class-II type in hepatitis B virus infection. *Nat. Genet.* **17**, 11-12 (1997).
5. Carrington, M. *et al.* HLA and HIV-1: Heterozygote advantage and B*35-Cw*04 disadvantage. *Science* **283**, 1748-1752 (1999).
6. Penn, D.J., Damjanovich, K. & Potts, W.K. MHC heterozygosity confers a selective advantage against multiple-strain infections. *Proc. Natl. Acad. Sci. USA* **99**, 11260-11264 (2002).
7. Savage, A.E. & Zamudio, K.R. MHC genotypes associate with resistance to a frog-killing fungus. *Proc. Natl. Acad. Sci. USA* **108**, 16705-16710 (2011).
8. Dean, M., Carrington, M. & O'Brien, S.J. Balanced polymorphism selected by genetic versus infectious human disease. *Annu. Rev. Genomics Hum. Genet.* **3**, 263-292 (2002).
9. Lipsitch, M., Bergstrom, C.T. & Antia, R. Effect of human leukocyte antigen heterozygosity on infectious disease outcome: the need for allele-specific measures. *BMC Med. Genet.* **4**, 2 (2003).

10. Woelfing, B., Traulsen, A., Milinski, M. & Boehm, T. Does intra-individual major histocompatibility complex diversity keep a golden mean? *Philos. Trans. R. Soc. Lond. B Biol. Sci.* **364**, 117-128 (2009).

11. Tsai, S. & Santamaria, P. MHC class II polymorphisms, autoreactive T-cells and autoimmunity. *Front. Immunol.* **4**, 321 (2013).

12. Goyette, P. *et al.* High-density mapping of the MHC identifies a shared role for HLA-DRB1*01:03 in inflammatory bowel diseases and heterozygous advantage in ulcerative colitis. *Nat. Genet.* **47**, 172-179 (2015).

13. Wordsworth, P. *et al.* HLA heterozygosity contributes to susceptibility to rheumatoid arthritis. *Am. J. Hum. Genet.* **51**, 585-91 (1992).

14. Thomson, G. *et al.* Relative predispositional effects of HLA class II DRB1-DQB1 haplotypes and genotypes on type 1 diabetes: a meta-analysis. *Tissue Antigens* **70**, 110-127 (2007).

15. Koeleman, B.P.C. *et al.* Genotype effects and epistasis in type 1 diabetes and HLA-DQ trans dimer associations with disease. *Genes Immun.* **5**, 381-388 (2004).

16. Wilkie, A.O. The molecular basis of genetic dominance. *J. Med. Genet.* **31**, 89-98 (1994).

17. Gjuvsland, A.B., Plahte, E., Ådnøy, T. & Omholt, S.W. Allele interaction – Single locus genetics meets regulatory biology. *PLoS ONE* **5**, e9379 (2010).

18. Lenz, T.L. Computational prediction of MHC II-antigen binding supports divergent allele advantage and explains trans-species polymorphism. *Evolution* **65**, 2380-2390 (2011).

19. Jia, X. *et al.* Imputing amino acid polymorphisms in human leukocyte antigens. *PLoS ONE* **8**, e64683 (2013).

20. Raychaudhuri, S. *et al.* Five amino acids in three HLA proteins explain most of the association between MHC and seropositive rheumatoid arthritis. *Nat. Genet.* **44**, 291-296 (2012).

21. Han, B. *et al.* Fine mapping seronegative and seropositive rheumatoid arthritis to shared and distinct HLA alleles by adjusting for the effects of heterogeneity. *Am. J. Hum. Genet.* **94**, 522-532 (2014).

22. Hu, X.Y. *et al.* Type 1 diabetes genetic risk, including multiple gene-gene interactions, maps to three amino acid positions encoded by the HLA-DQB1 and HLA-DRB1 genes. (Submitted).

23. Okada, Y. *et al.* Fine mapping major histocompatibility complex associations in psoriasis and its clinical subtypes. *Am. J. Hum. Genet.* **95**, 162-172 (2014).

24. Gockel, I. *et al.* Common variants in the HLA-DQ region confer susceptibility to idiopathic achalasia. *Nat. Genet.* **46**, 901-904 (2014).

25. Gutierrez-Achury, J. *et al.* Fine-mapping in the MHC region accounts for 18% additional genetic risk for celiac disease. (In review).

26. Rich, S.S. *et al.* The Type 1 Diabetes Genetics Consortium. *Ann. N. Y. Acad. Sci.* **1079**, 1-8 (2006).

27. Eyre, S. *et al.* High-density genetic mapping identifies new susceptibility loci for rheumatoid arthritis. *Nat. Genet.* **44**, 1336-1340 (2012).

28. Balding, D.J., Bishop, M.J. & Cannings, C. *Handbook of statistical genetics*, (John Wiley & Sons, Chichester, UK, 2007).

29. Stahl, E.A. *et al.* Bayesian inference analyses of the polygenic architecture of rheumatoid arthritis. *Nat. Genet.* **44**, 483-9 (2012).

30. de Bakker, P.I.W. *et al.* Practical aspects of imputation-driven meta-analysis of genome-wide association studies. *Hum. Mol. Genet.* **17**, R122-R128 (2008).

31. Clop, A. *et al.* An in-depth characterization of the major psoriasis susceptibility locus identifies candidate susceptibility alleles within an *HLA-C* enhancer element. *PLoS ONE* **8**, e71690 (2013).

32. Gregersen, P.K., Silver, J. & Winchester, R.J. The shared epitope hypothesis. an approach to understanding the molecular genetics of susceptibility to rheumatoid arthritis. *Arthritis. Rheum.* **30**, 1205-1213 (1987).

33. Holoshitz, J. The rheumatoid arthritis HLA–DRB1 shared epitope. *Curr. Opin. Rheumatol.* **22**, 293–298 (2010).

34. MacGregor, A., Ollier, W., Thomson, W., Jawaheer, D. & Silman, A. HLA-DRB1*0401/0404 genotype and rheumatoid arthritis: increased association in men, young age at onset, and disease severity. *J. Rheumatol.* **22**, 1032-6 (1995).

35. Megiorni, F. & Pizzuti, A. HLA-DQA1 and HLA-DQB1 in Celiac disease predisposition: practical implications of the HLA molecular typing. *J. Biomed. Sci.* **19**, 1-5 (2012).

36. Vader, W. *et al.* The HLA-DQ2 gene dose effect in celiac disease is directly related to the magnitude and breadth of gluten-specific T cell responses. *Proc. Natl. Acad. Sci.* **100**, 12390-12395 (2003).

37. Monsuur, A.J. *et al.* Effective detection of human leukocyte antigen risk alleles in celiac disease using tag single nucleotide polymorphisms. *PLoS ONE* **3**, e2270 (2008).

38. Klareskog, L., Lundberg, K. & Malmström, V. Autoimmunity in rheumatoid arthritis: Citrulline immunity and beyond. in *Advances in Immunology*, Vol. 118 (ed. Frederick, W.A.) 129-158 (Academic Press, 2013).

39. Viatte, S., Plant, D. & Raychaudhuri, S. Genetics and epigenetics of rheumatoid arthritis. *Nat. Rev. Rheumatol.* **9**, 141-153 (2013).

40. Miyadera, H. *et al.* Cell-surface MHC density profiling reveals instability of autoimmunity-associated HLA. *J. Clin. Investig.* **125**, 275-291 (2015).

METHODS

Samples

We analyzed genotype data from previously published studies of HLA association in anti-citrullinated protein antibody positive ($ACPA^+$) rheumatoid arthritis (RA, N = 16,386)[21], type 1 diabetes (T1D, N = 11,832)[22], psoriasis vulgaris (PsV, N = 9,053)[23], idiopathic achalasia (Ach, N = 3,638)[24], and celiac disease (CeD, N = 20,157)[25]. Each dataset contained samples from multiple case-control GWAS cohorts, and all individuals had European ancestry (**Supplementary Table S1**).

HLA genotypes and imputation quality

The SNP genotype data for the MHC region, obtained from previous disease-specific studies (see above), was generated by the Illumina ImmunoChip platform[41]. Following previous studies, we defined the MHC region as the region on chromosome 6 from 29Mb to 34Mb. Stringent quality control was conducted following the disease-specific studies described above. We imputed four-digit classical HLA alleles with SNP2HLA[19], using dense SNP data across the MHC region for each disease dataset (number of SNPs used for imputation for RA: 4,499; for T1D: 4,604; PsV: 4,030; for Ach: 3,773; and for CeD: 3,249) and a reference panel of 5,225 individuals of European ancestry from the Type 1 Diabetes Genetics Consortium (T1DGC)[26]. We have separately demonstrated high imputation accuracy using genotype data from the ImmunoChip platform[19].

For each allele, the INFO score was calculated from the ratio of the observed variance in dosage to the expected variance under Hardy-Weinberg equilibrium[30]:

$$I \quad N = \frac{\mathrm{V} \quad x)}{2(p)\ 1-\ell} \quad \text{(Equation 1)}$$

where *x* is the imputed dosage and *p* is the frequency of the allele. An INFO score close to 0 indicates poor imputation quality, while a score closer to 1 indicates higher quality; a value greater than 1 is also possible. Due to the presence of non-additive effects that inflated the disease risk in heterozygotes, the allele distribution in disease cases deviated from Hardy-Weinberg equilibrium. Therefore, we calculated INFO scores using the variance and allele frequency in controls only (**Supplementary Table S2**). However, because the imputation algorithm does not take case/control status into account, we expected that imputation quality should be similar in cases and controls. For RA, we also calculated INFO scores within each cohort to test whether lower INFO scores (i.e. lower quality of imputed genotypes) were associated with a higher likelihood to detect non-additive effects, which could suggest that non-additive effects are an artifact of imputation errors.

Selection of genes for analysis

For each disease, we selected the HLA genes that were most significantly associated with disease risk in previous studies (RA: *HLA-DRB1*[21]; T1D: *HLA-DRB1, HLA-DQA1*, *HLA-DQB1*[22]; PsV: *HLA-C*[23]; Ach: *HLA-DQA1, HLA-DQB1*[24]; CeD: *HLA-DQA1, HLA-DQB1*[25]). For diseases in which more than one HLA gene was implicated to confer major independent risk contribution, we defined haplotypes according to unique combinations of four-digit classical alleles at each relevant gene. We used phased best guess genotypes from SNP2HLA to ensure that each haplotype contained classical alleles on the same chromosome.

For RA and PsV, we repeated the analysis using imputed dosages (which range on a continuous scale from 0-2) rather than best guess genotypes (which are restricted to the integer values 0, 1, or 2; see **Supplementary Table S5**). Because imputed dosages do not contain phasing information, we did not perform this analysis for the diseases involving multiple genes.

Selection of alleles for analysis

We performed all association tests with two datasets: the common allele dataset and the full dataset. In the common allele dataset, we restricted our analysis to classical alleles with a frequency greater than or equal to 5% in the T1DGC reference panel, or haplotypes comprising these classical alleles (RA: $m = 5$; T1D: $m = 5$; PsV: $m = 7$; Ach: $m = 5$; CeD: $m = 6$; where m indicates the number of included HLA alleles/haplotypes). This cutoff ensured a very high imputation quality, and INFO scores for all alleles in the common allele subset exceeded 0.97 (**Supplementary Table S2**). We also ensured that all haplotypes in the common subset had at least 10 homozygous individuals. (If fewer than 10 homozygotes are present, the additive and non-additive terms are statistically indistinguishable.) In the full dataset, we included all m variants (four-digit classical alleles or haplotypes) with at least 10 homozygous individuals (RA: $m = 11$; T1D: $m = 11$; PsV: $m = 13$; Ach: $m = 9$; CeD: $m = 10$).

We ensured complete data in both datasets by excluding all individuals who lacked exactly two best-guess alleles at a given locus. For analyses that used imputed dosages, we excluded all individuals whose total dosage across the relevant alleles was less than 1.95 or greater than 2.05.

Statistical framework for association testing

To analyze the effects of HLA haplotypes on disease risk, we used a logistic regression framework. We began by presenting a baseline model, consistent with the models used to fine-map HLA effects in previous recent publications for RA[21], T1D[22], PsV[23], Ach[24], and CeD[25]. These models assume a purely additive contribution from each haplotype. To control for cohort-specific effects and population stratification, we included an indicator variable for each cohort, the first *L* principal components (for RA, PsV, and Ach), and a gender term (for T1D and CeD) as covariates. This resulted in the following logistic regression model:

$$\log(odds_i) = \theta + \sum_{j=1}^{m-1} a_j x_{i,j} + \sum_{k=1}^{K} \delta_{i,k}(\lambda_k + \sum_{l=1}^{L} \pi_{k,l} p_{i,k,l}) + \gamma g_i \quad \text{(Equation 2)}$$

where θ is the logistic regression intercept, a_j is the additive effect of allele *j*, and $x_{i,j}$ is the allelic dosage (using best guess genotype or imputed dosage) of allele *j* in individual *i*. For a multi-allelic locus with *m* possible alleles, we included *m* – 1 *a* parameters, and we set the final *a* parameter to 0 to denote the reference allele. We arbitrarily selected the most common allele in the controls as the reference allele. The parameter $\delta_{i,k}$ is a binary indicator variable that equals 1 if and only if individual *i* is in cohort *k*, and λ_k is the effect for the k^{th} cohort. Among a total of *K* cohorts, we arbitrarily selected the largest cohort as the reference cohort and set its λ parameter to 0.

For RA, PsV, and Ach, we also included the first *L* principal components, where $p_{i,k,l}$ is the value of principal component *l* in cohort *k* for individual *i*, and $\pi_{k,l}$ is the corresponding effect size. To be consistent with HLA fine mapping studies on other diseases, we used *L* = 10 for RA[21] and PsV[23], *L* = 5 for Ach[24], and no principal components for T1D[22] or for CeD[25].

We included an additional covariate to account for gender differences in T1D and CeD, once again to conform to previous HLA fine-mapping analyses[22,25]. Here, γ is the effect of gender, and g_i is a binary indicator variable that equals 1 if and only if individual *i* is female. We did not include the g_i parameter for RA, PsV, or Ach, following refs. [21],[23], and [24], respectively.

We tested significance in fit for each model by calculating the change in deviance (defined as -2 × the difference in log likelihood) from the original model to the revised model. This value follows a χ^2 distribution with *n* degrees of freedom, where *n* is the number of new parameters introduced in the revised model. For the additive model, *n* is 1 less than the total number of tested haplotypes (to account for a reference haplotype).

Analysis of dominance and interaction effects

For each disease, we tested for non-additive effects by including a dominance term d_j for each represented haplotype in the relevant dataset (the common allele subset or the full dataset):

$$\log(\text{odds}) = \theta + \sum_{j=1}^{m-1} a_j x_{i,j} + \sum_{j=1}^{m} d_j \delta_{x_{i,j}} + \sum_{k=1}^{K} \delta_{i,k}(\lambda_k + \sum_{l=1}^{L} \pi_{k,l} p_{i,k,l}) + \gamma g_i \quad \text{(Equation 3)}$$

where d_j represents the dominance effect of allele *j*, and $\delta_{xi,j}$ denotes that individual *i* is heterozygous for haplotype *j*. For analyses involving best guess genotypes, $\delta_{xi,j}$ if and only if $x_{i,j} = 1$. For dosage-based analyses, we used the formula $\delta_{xi,j} = 1 - \text{abs}(1 - x_{i,j})$. We assessed the change in deviance between the additive model and the dominance model, which follows a χ^2 distribution with *m* degrees of freedom (1 for each haplotype). To determine the relative non-additive effect of a specific haplotype, we constructed a separate model for each haplotype by repeating the model in

equation 3 for a single value of *j* (1 degree of freedom). For the single-haplotype models, we used a significance threshold of $P < 0.05/m$ to correct for multiple tests.

We also constructed an interaction model, which contains an additive term for each haplotype and an interaction term between each pair of haplotypes:

$$\log(odds_i) = \theta + \sum_{j=1}^{m-1} a_j x_{i,j} + \sum_{j=1}^{m} \sum_{h=j+1}^{m} \phi_{j,h} x_{i,j} x_{i,h} + \sum_{k=1}^{K} \delta_{i,k} (\lambda_k + \sum_{l=1}^{L} \pi_{k,l} p_{i,k,l}) + \gamma g_i \quad \text{(Equation 4)}$$

where $\phi_{j,h}$ is effect size of the interaction between alleles *j* and *h*. We did not include dominance terms in this model, due to partial redundancy between dominance and interaction terms. The interaction model contains an additional $m(m-1)/2$ degrees of freedom (1 for each pairwise interaction), compared to the additive model. We assessed the change in deviance between the dominance model and the interaction model, which follows a χ^2 distribution with $m(m-1)/2 - m$ degrees of freedom. To determine the relative significance of individual interaction terms, we compared the *P*-values associated with each ϕ parameter, and we used a significance threshold of $P < 0.05 / [m(m-1)/2]$.

To compare the disease risk in homozygotes and heterozygotes, we constructed additive models after excluding all homozygous individuals (to estimate the heterozygous effect size) or excluding all heterozygous individuals (to estimate the homozygous effect size). For dosage-based analyses, we defined heterozygous individuals as those with a dosage greater than 0.95 and less than or equal to 1.05, while homozygous individuals were those with a dosage greater than 1.05.

Calculation of phenotypic variance explained

We separately calculated the percent of phenotypic variance explained at each locus, as described previously[20,42]. We used a model based on the biometrical model from Fisher[43] and the liability threshold model from Pearson and Lee[44]. We assumed that disease risk is the consequence of an underlying liability score that is normally distributed with a mean of zero and a variance of one, and that individuals with a score above a pre-specified threshold get disease[45]. We determined the thresholds by assuming the following prevalence for each disease: RA = 0.5%[46], T1D = 0.4%[47], PsV = 2%[48], Ach = 0.01%[24], and CeD = 1%[35]. We also assumed that genetic factors can alter these thresholds.

To investigate the percent variance explained by a single locus, we determined the prevalence of disease for individuals with each possible genotype, which is approximately equal to the population frequency multiplied by the effect size of the given genotype. We then determined the corresponding change in the liability score threshold for each genotype. The distance between the thresholds represents the change in the genotypic means, and we calculated the variance attributable to the locus by taking the average squared difference in means, weighted by genotypic frequency. For each allele, we assumed that the population frequency was equal to the average control frequency. We assumed that the effect size of each genotype was the odds ratio derived from one of the three models used in our study: the additive model, the additive plus non-additive model, or the additive plus interactions model (for RA, T1D, and CeD only).

Analysis of amino acid-level non-additive effects

For RA, we also analyzed non-additive effects of individual amino acid positions within specific HLA genes. We used imputed amino acid genotypes at positions 13,

71, and 74 of HLA-DRB1, and we analyzed all residues at these positions with a frequency greater than or equal to 5% in the T1DGC reference panel. We used the previously described allele-level models (**Equations 2 and 3**) to assess the non-additive effects of amino acid variants.

Because amino acid positions within a given locus are very tightly linked, we used a stepwise conditioning approach to test the effects at successive positions on RA risk, following refs. [20,49]. We analyzed positions in the order of significance of additive contribution to disease risk. First, we analyzed non-additive effects in DRB1-13. Then, we analyzed DRB1-71 while conditioning on DRB1-13, and we analyzed DRB1-74 while conditioning on DRB1-13 and DRB1-71. To condition on a specific amino acid position, we included all possible amino acid variants at that position as covariates, but we excluded any variant that had strong correlations to other variants in the dataset ($R^2 > 0.97$)[23].

Permutation of imputed HLA genotypes

To verify that the observed non-additive effects were not a subtle artifact of imputation inaccuracies, we permuted SNP-imputed HLA genotypes across cases and controls, based on the case probability predicted by a purely additive model (**Equation 2**). This approach conserves allele frequencies (which confer additive disease associations) within cases and controls and also conserves individual genotypes. However, it randomizes the distribution of homozygote and heterozygote genotypes among cases and controls. We performed 10,000 permutations, and for each permutation we recorded the deviance of a non-additive model with dominance terms for all relevant HLA haplotypes (**Equation 3**). To validate the permuted cohorts, we also compared the distribution of additive effects for each relevant HLA

haplotype with the observed values in the actual dataset (**Supplementary Figure S3**).

Method references

41. Trynka, G. *et al.* Dense genotyping identifies and localizes multiple common and rare variant association signals in celiac disease. *Nat. Genet.* **43**, 1193-1201 (2011).

42. Raychaudhuri, S. *et al.* Common variants at CD40 and other loci confer risk of rheumatoid arthritis. *Nat. Genet.* **40**, 1216-1223 (2008).

43. Fisher, R.A. The correlation between relatives on the supposition of mendelian inheritance. *Trans. R. Soc. Edinb.* **52**, 399-433 (1919).

44. Pearson, K. & Lee, A. On the inheritance of characters not capable of exact quantitative measurement. *Philos. Trans. R. Soc. Lond. A* **195**, 79-150 (1900).

45. Kwan, S.H., Purcell, S. & Sham, P.C. Biometrical Genetics. in *Statistical Genetics: Genemapping through linkage and association* (eds. Neale, B.M., Ferreira, M.A.R., Medland, S.E. & Posthuma, D.) (Taylor & Francis, London, UK, 2007).

46. Helmick, C.G. *et al.* Estimates of the prevalence of arthritis and other rheumatic conditions in the United States. Part I. *Arthritis Rheumatol.* **58**, 15-25 (2008).

47. Maahs, D.M., West, N.A., Lawrence, J.M. & Mayer-Davis, E.J. Epidemiology of type 1 diabetes. *Endocrinol. Metab. Clin. N. Am.* **39**, 481-97 (2010).

48. Langley, R.G.B., Krueger, G.G. & Griffiths, C.E.M. Psoriasis: epidemiology, clinical features, and quality of life. *Ann. Rheum. Dis.* **64**, ii18-ii23 (2005).

49. Okada, Y. *et al.* Risk for ACPA-positive rheumatoid arthritis is driven by shared HLA amino acid polymorphisms in Asian and European populations. *Hum. Mol. Genet.* **23**, 6916-6926 (2014).

Tables

Table 1

Disease	Loci				Additive model			Non-additive model (add. + non-add. component)				
					P	OR	95% CI	*P*	Heterozygote effect		Homozygote effect	
	HLA-C	HLA-DRB1	HLA-DQA1	HLA-DQB1					OR	95% CI	OR	95% CI
RA		01:01			$1.6x10^{-22}$	1.54	(1.41-1.68)	$1.3x10^{-8}$	1.77	(1.61-1.96)	1.17	(0.87-1.58)
		04:01			$2.0x10^{-206}$	3.31	(3.05-3.59)	$1.4x10^{-7}$	3.93	(4.36-8.34)	8.34	(6.87-10.12)
		03:01			$1.2x10^{-51}$	0.50	(0.45-0.55)	$8.6x10^{-4}$	0.54	(0.61-0.15)	0.15	(0.10-0.22)
		15:01			$7.7x10^{-43}$	0.55	(0.51-0.60)	$1.2x10^{-3}$	0.60	(0.67-0.21)	0.21	(0.15-0.28)
T1D		07:01	02:01	02:02	$4.2 x10^{-50}$	0.38	(0.33-0.43)	$1.9x10^{-5}$	0.32	(0.28-0.37)	0.31	(6.39-9.01)
		04:01	03:01	03:01	$2.2x10^{-167}$	0.18	(0.16-0.21)	$3.4x10^{-5}$	0.20	(0.18-0.23)	0.004	(0.001-0.018)
		04:01	03:01	03:02	$5.4x10^{-224}$	6.09	(5.38-6.90)	$3.5x10^{-5}$	6.72	(5.88-7.68)	13.86	(8.79-21.86)
		03:01	05:01	02:01	$5.2x10^{-35}$	1.70	(1.56-1.85)	$3.5x10^{-3}$	1.92	(1.71-2.16)	2.55	(2.12-3.08)
PsV	06:02				$1.5x10^{-92}$	2.94	(2.65-3.28)	$4.9x10^{-8}$	3.49	(3.09-3.95)	4.28	(3.11-5.87)
CeD			02:01	02:02	$1.3 x10^{-67}$	1.86	(1.73-1.99)	$6.7x10^{-62}$	2.36	(2.18-2.55)	0.36	(0.27-0.50)
			05:01	03:01	$5.3x10^{-156}$	0.35	(0.32-0.38)	$3.0x10^{-25}$	0.42	(0.39-0.46)	0.03	(0.02-04)
			05:01	02:01	$4.3x10^{-675}$	5.78	(5.38-6.20)	$4.7x10^{-19}$	7.28	(6.67-7.95)	22.80	(19.43-26.75)
			03:01	03:02	$8.5x10^{-67}$	0.50	(0.46-0.54)	$3.5x10^{-11}$	0.43	(0.39-0.47)	0.55	(0.42-0.73)
			01:01	05:01	$4.0x10^{-216}$	0.27	(0.25-0.29)	$3.2x10^{-6}$	0.29	(0.26-0.32)	0.02	(0.01-0.04)

Table 1: Effect sizes of common HLA haplotypes with significant non-additive effects. Additive and non-additive effect sizes are shown for all haplotypes with significant non-additive disease contribution in RA (*HLA-DRB1*), T1D (*HLA-DRB1-DQA1-DQB1*), PsV (*HLA-C*), and CeD (*HLA-DQA1-DQB1*). For diseases associated with multiple HLA loci, linked classical alleles across those loci were analyzed as haplotypes. *P*-values indicate the significance of improvement in fit by haplotype-specific models after sequentially including the additive and the non-additive term for a given haplotype. Odds ratios (OR)

and 95% confidence intervals (CI) are given for a purely additive scenario and for a non-additive scenario, in which heterozygotes and homozygotes have separate effects. Haplotypes are ordered by significance of the non-additive effect within each dataset.

Table 2

(a) RA

	DRB1	01:01	03:01	04:01	07:01	15:01
DRB1	Additive OR	1.96	0.84	3.84	0.82	1.00 (Ref)
15:01	1.00 (Ref)	**2.06 (1.6×10^{-7})**	1.50 (0.02)	**1.43 (1.8×10^{-3})**	1.27 (0.20)	
07:01	0.82	**2.02 (8.9×10^{-6})**	1.03 (0.89)	**1.49 (3.6×10^{-3})**		
04:01	3.84	**1.87 (2.9×10^{-8})**	**1.92 (5.2×10^{-7})**			
03:01	0.84	**1.63 (2.2×10^{-3})**				
01:01	1.96					

(b) CeD

	DQA1-DQB1	01:01 05:01	02:01 02:02	03:01 03:01	03:01 03:02	05:01 02:01	05:01 03:01
DQA1-DQB1	Additive OR	0.86	2.76	0.79	4.53	13.03	1.00 (Ref)
05:01 03:01	1.00 (Ref)	1.14 (0.67)	**16.85 (7.0×10^{-74})**	2.04 (0.12)	0.98 (0.91)	**2.05 (2.2×10^{-7})**	
05:01 02:01	13.03	**3.74 (1.9×10^{-10})**	**4.36 (2.4×10^{-44})**	0.71 (0.37)	0.79 (0.03)		
03:01 03:02	4.53	1.08 (0.75)	1.23 (0.15)	1.05 (0.90)			
03:01 03:01	0.79	1.42 (0.51)	1.53 (0.32)				
02:01 02:02	2.76	1.08 (0.77)					
01:01 05:01	0.86						

Table 2: Interaction effects among HLA haplotypes. Pairs of common haplotypes with significant interaction effects are shown for **(a)** RA (*HLA-DRB1*) and **(b)** CeD (*HLA-DQA1-DQB1*). The odds ratio (OR) is displayed for each interaction, and the *P*-value associated with each odds ratio is shown in parentheses. Additive ORs are also displayed for each haplotype, shaded in light gray. All ORs and *P*-values were obtained from a global disease model with an additive term for each haplotype and an interaction term for each pair of haplotypes. ”Ref” indicates the reference haplotype for each regression model. Bolded values indicate interactions that are significant after multiple test correction ($P < 0.05/10 = 0.005$ for RA, $P < 0.05/15 = 0.003$ for CeD)

Figures

Figure 1

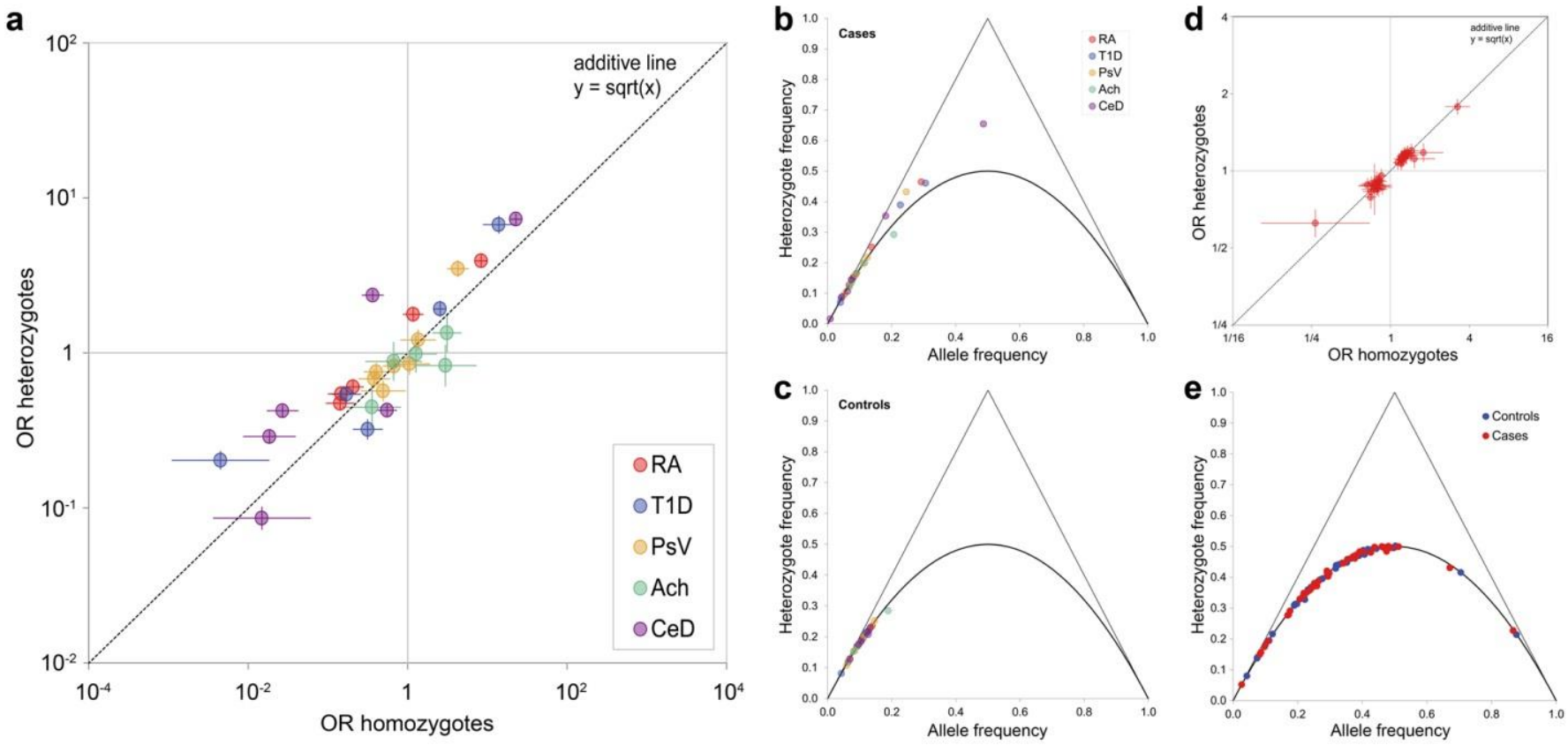

Figure 1. Disease associations of HLA and non-HLA variants. (a) Disease associations of HLA haplotypes with RA, T1D, PsV, Ach, and CeD. For each common haplotype, the odds ratio (OR) for heterozygotes is plotted against the OR for homozygotes. The dashed line represents a purely log-additive relationship, in which heterozygotes have exactly half the risk

of homozygotes (on a log-odds scale). Data points above the dashed line represent haplotypes with a positive dominance component, and below the line haplotypes with a negative dominance component. Error bars represent 95% confidence intervals. **(b,c)** De Finetti diagram of the proportion of heterozygotes in relation to the frequency of each HLA haplotype (grouped across all diseases), shown separately for **(b)** cases and **(c)** controls. The solid line represents the expected proportion of heterozygotes under Hardy-Weinberg-Equilibrium. **(d)** Disease association of 44 known genome-wide RA-associated SNPs located outside the MHC region, using the same plotting scheme as for panel **a**. No single SNP shows a significant deviation from the dashed line (representing a purely additive disease contribution). **(e)** De Finetti diagram of heterozygote frequency for the same 44 non-MHC SNPs as in panel **d**, given separately for controls and cases.

Figure 2

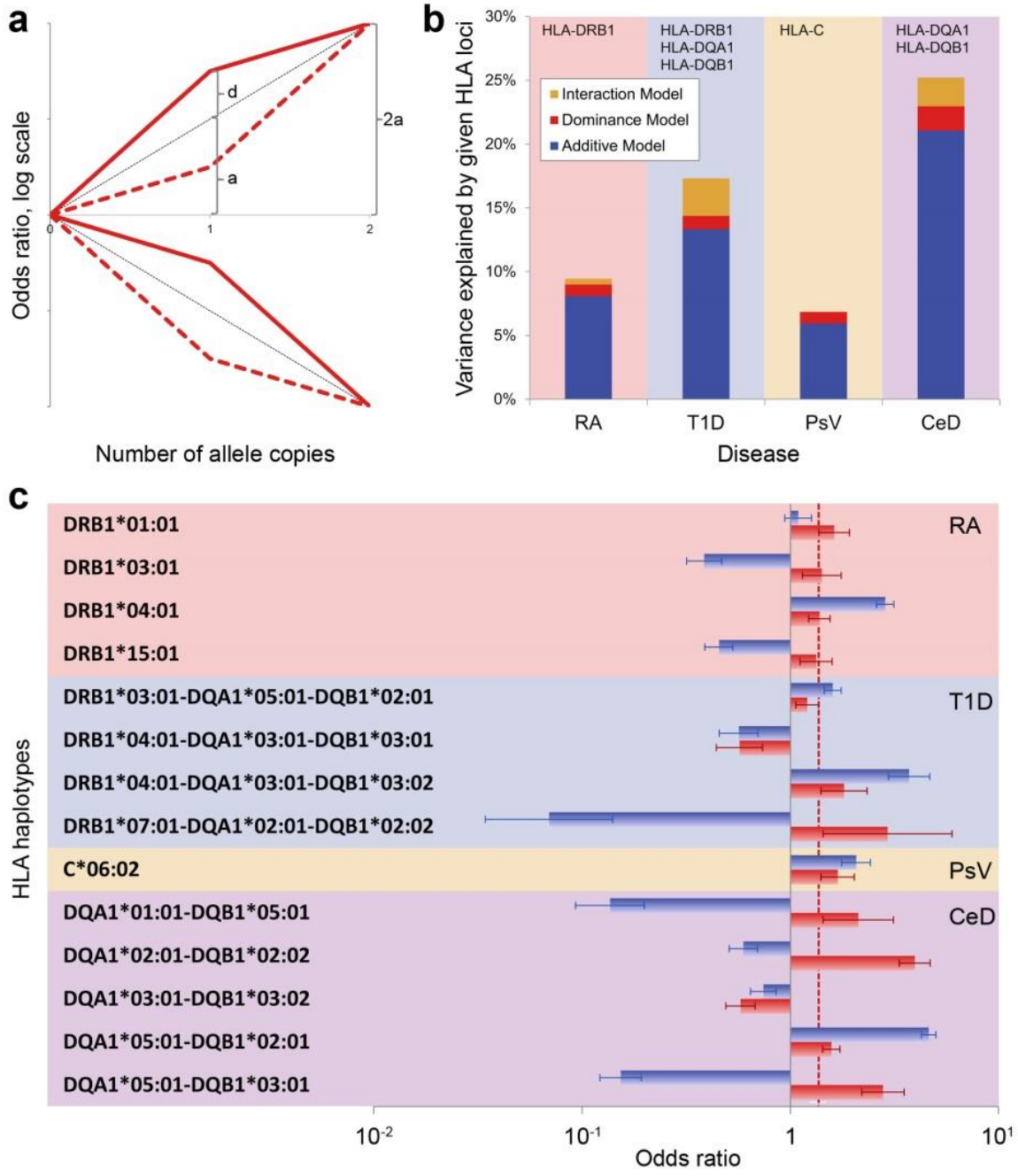

Figure 2: Non-additive contribution of the HLA to autoimmune disease risk. (a) Schematic overview of possible non-additive scenarios. The log-odds for heterozygote genotypes can be divided into an additive effect *a* and a dominance component *d*, which represents the departure from additivity. Depending on the signs of *a* and *d*, there are

four possible scenarios, represented by red lines. Dashed black lines represent the expected log-odds under a purely additive model ($d = 0$). As an example, the values of a and d are indicated for the solid red line (risk variant with positive dominance component). (**b**) Phenotypic variance explained by additive, dominant, and interaction effects of HLA haplotypes, respectively, for each disease with a significant non-additive HLA contribution (RA, T1D, PsV, CeD). **(c)** For each common HLA haplotype with significant non-additive effect in RA, T1D, PsV, and CeD, we calculated the additive (blue bars) and dominance (red bars) components of the log-odds for heterozygotes. The dashed line indicates the median of the dominance components depicted in the figure. Error bars represent 95% confidence intervals.

Figure 3

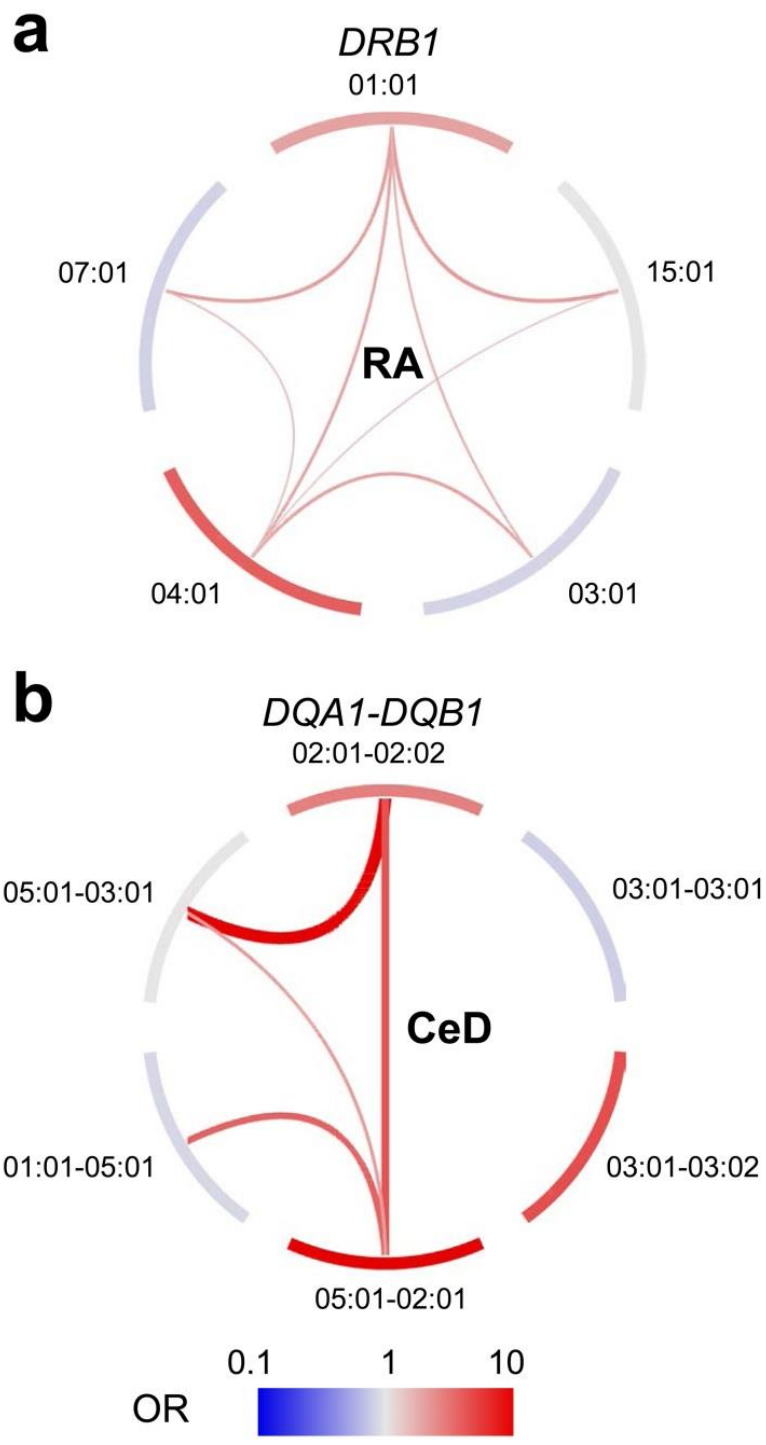

Figure 3: Interaction effects in the HLA. All common HLA haplotypes (frequency > 5%) are displayed for **(a)** HLA-DRB1 (RA) and **(b)** HLA- DQA1/DQB1 (CeD). Nodes represent haplotypes with the color indicating their additive disease contribution, while

edges represent significant interaction effects. For both nodes and edges, red color indicates disease risk and blue indicates protection, with effect sizes following the scale at the bottom. The effect sizes of the interactions are also represented by the width of the edges.